Applied Physics Letters

Phase transition of Al_2O_3-encapsulated $MoTe_2$ via rapid thermal annealing

Cite as: Appl. Phys. Lett. **121**, 033101 (2022); https://doi.org/10.1063/5.0097844
Submitted: 02 May 2022 • Accepted: 05 July 2022 • Published Online: 19 July 2022

Rohan Sengupta, Saroj Dangi, Sergiy Krylyuk, et al.

Applied Physics Letters ARTICLE scitation.org/journal/apl

Phase transition of Al_2O_3-encapsulated $MoTe_2$ via rapid thermal annealing

Cite as: Appl. Phys. Lett. **121**, 033101 (2022); doi: 10.1063/5.0097844
Submitted: 2 May 2022 · Accepted: 5 July 2022 ·
Published Online: 19 July 2022

Rohan Sengupta,[1] Saroj Dangi,[1] Sergiy Krylyuk,[2] Albert V. Davydov,[2] and Spyridon Pavlidis[1,a)]

AFFILIATIONS

[1]Department of Electrical and Computer Engineering, North Carolina State University, Raleigh, North Carolina 27695-7911, USA
[2]Materials Science and Engineering Division, National Institute of Standards and Technology, Gaithersburg, Maryland 20899, USA

[a)]Author to whom correspondence should be addressed: spavlidis@ncsu.edu

ABSTRACT

Among group VI transition metal dichalcogenides, $MoTe_2$ is predicted to have the smallest energy offset between semiconducting 2H and semimetallic 1T′ states. This makes it an attractive phase change material for both electronic and optoelectronic applications. Here, we report fast, nondestructive, and full phase change in Al_2O_3-encapsulated 2H-$MoTe_2$ thin films to 1T′-$MoTe_2$ using rapid thermal annealing at 900 °C. Phase change was confirmed using Raman spectroscopy after a short annealing duration of 10 s in both vacuum and nitrogen ambient. No thickness dependence of the transition temperatures was observed for flake thickness ranging from 1.5 to 8 nm. These results represent a major step forward in understanding the structural phase transition properties of $MoTe_2$ thin films using external heating and underline the importance of surface encapsulation for avoiding thin film degradation.

$MoTe_2$ is predicted to have the smallest energy offset between the trigonal prismatic semiconducting 2H structure and the distorted octahedral semimetallic 1T′ structure among the group VI transition metal dichalcogenides (TMDs).[1] This, along with the 2D layered nature of $MoTe_2$, makes it a promising candidate as a phase change material (PCM) for low-power nonvolatile switches in high density memory applications,[2] reconfigurable RF modules,[3] and neuromorphic computing.[4,5] Moreover, a thickness-dependent bandgap of ≈1 eV highlights the possibility of 2H-$MoTe_2$ to be used in tunable optical filters and photodetectors in the near infrared region.[9–11] It should be noted that not all applications demand repeatable and reversible phase change. For example, the local and nonreversible phase change of 2H-$MoTe_2$ to 1T′-$MoTe_2$ has been proposed in order to improve contact resistance to the source and drain regions of lateral channel transistors.[6–8] To fulfill its potential in these applications, a fundamental understanding of the conditions that trigger the 2H to 1T′ phase transition in $MoTe_2$ must first be established.

A variety of experimental methods have been attempted to induce this transition. Experimental results for phase control of $MoTe_2$ during the growth process have been reported wherein the growth temperature and cooling rate,[12–14] the tellurization flux rate,[7,15] and the choice of a growth substrate[16] can all be tuned. While important for material synthesis, these approaches cannot be adopted for all device applications. Wang *et al.*[17] demonstrated the 2H to 1T′ structural phase change in monolayer $MoTe_2$ films driven by ionic liquid gating, where they used Raman spectroscopy and the second harmonic generation to show the reversibility of such phase transition. This approach was further extended to multilayer 2H-$MoTe_2$ films by Zakhidov *et al.*[18] to attempt phase transition at room temperature; in air, it did not lead to the complete phase change, with the 2H and 1T′ phases coexisting for $MoTe_2$ films thicker than a monolayer. It also resulted in the formation of Te vacancies via electrochemical reactions on the $MoTe_2$ surface. While ionic liquid gating is a useful method to investigate material properties, this approach cannot be utilized in practical device applications due to integration and stability issues.[19,20] Strain[21] and laser heating[22,23] have also been used to attempt phase change from 2H to 1T′. Although Raman spectroscopy has previously been used to confirm the change of phase in the $MoTe_2$ films,[21–23] the report by Chen *et al.*[24] on intrinsic phonon bands of high quality 1T′-$MoTe_2$ raises question regarding the final product achieved in the above-mentioned papers, since the Raman peaks assigned to the 1T′ phase in those studies are similar to the Te metalloid Raman modes, which is a by-product of sample degradation. Hou *et al.*[25] used a ferroelectric substrate to modulate the conductance of 1T′-$MoTe_2$, demonstrating a drop in conductance compared to the initial 1T′ film. Hydrogen plasma treatment has also been reported to change the electrical conductivity of $MoTe_2$ thin films, but no clear demonstration of structural phase transition was made in that report.[26] Zhang *et al.*

demonstrated the ability to induce a phase transition from the semiconducting 2H to a higher conductivity distorted transient phase $2H_d$ via the application of an electrical field in vertical $MoTe_2$ devices.[27]

Thermal actuation of GeTe-based PCM switches has been studied for a long time, where an inline heater is used to trigger a fast (on a μs-timescale) amorphous–crystalline phase change.[3,28] The thermally driven 2H–1T′ crystalline–crystalline phase transition in $MoTe_2$ appears to be much slower. In our experiments, the 2H–1T′ transition in bulk $MoTe_2$ was achieved after about 24 h vacuum annealing at 970 °C (not shown). Recently, Ryu *et al.*[6] demonstrated phase transition of h-BN encapsulated exfoliated 2H-$MoTe_2$ using high temperature vacuum annealing (1000 °C) and long annealing times of 3 h.

In this work, we study the thermally driven and nondestructive phase transition in $MoTe_2$ from semiconducting 2H to semimetallic 1T′ via rapid thermal annealing (RTA). We report a phase change temperature of 900 °C using Al_2O_3 as an encapsulation layer. We observe the phase change in a much shorter annealing duration of 10 s, in both vacuum and N_2 ambient. We demonstrate that capping the $MoTe_2$ with Al_2O_3 is crucial to preserving materials' integrity and consequently inducing a phase transition. These results help to understand phase transitions in van der Waals layered materials and move $MoTe_2$ closer toward practical use in optoelectronic and electronic applications.

The 2H to 1T′ phase transition was studied in Al_2O_3-capped $MoTe_2$ exfoliated films as shown in Fig. 1. Bulk single crystals of $MoTe_2$ were fabricated using the chemical vapor transport (CVT) method. Polycrystalline $MoTe_2$ powder was sealed in evacuated quartz ampoules with a small amount of I_2 (5 mg/cm^3), which served as a transport agent. The ampoules were annealed at 950 °C to 1000 °C for seven days, followed by cooling to room temperature at a rate of 10–20 °C/h to stabilize the 2H phase. The 1T′ phase was stabilized by ice water quenching.

$MoTe_2$ thin films of each phase were mechanically exfoliated from the bulk crystals on a 300 nm thick SiO_2 layer on high conductivity p^{++}-Si wafers using the Scotch tape technique. The wafers were annealed at 300 °C in N_2 ambient to remove tape residues. 2 nm of aluminum was thermally evaporated and then allowed to oxidize in air to form an oxide layer, which acts as a seeding layer for the subsequent deposition of a 10 nm Al_2O_3 capping layer using plasma atomic layer deposition (ALD) at 150 °C.[29] The capped $MoTe_2$ structures were then put in the RTA furnace (Annealsys RTP) for the annealing experiments. The RTA is ramped up at a rate of 10 °C/s followed by 10 s of dwell time at 900 °C. The system then rapidly cools down to room temperature in less than 5 min [Fig. 1(b)].

We performed Raman spectroscopy (Horiba XPloRA PLUS) using a 532 nm laser at low power of 2.5 mW on exfoliated 2H and 1T′ flakes before and after capping with Al_2O_3. Raman spectroscopy was also used to monitor the phase of the $MoTe_2$ films after the annealing experiments. We also performed x-ray diffraction (XRD) on our exfoliated samples before the RTA process to confirm the crystal structure of $MoTe_2$. Tapping mode atomic force microscope (AFM) (MFP-3D) was used to determine the thickness of the $MoTe_2$ flakes.

The Raman spectra of as-exfoliated and Al_2O_3-capped $MoTe_2$ thin films were measured prior to RTA. As shown in Fig. 2(a), the observed peaks are consistent with the characteristic phonon modes of each phase. For 2H-$MoTe_2$, these are the A_{1g} mode at 170 cm^{-1}, E_{2g} mode at 234 cm^{-1}, and B_{2g} mode at 289 cm^{-1}.[30] The B_{2g} mode is absent in bulk but is observed in few layer 2H-$MoTe_2$ due to breaking of translational symmetry of the crystal. The characteristic phonon modes of 1T′-$MoTe_2$ are the A_g modes located at 109, 126, 162, and 257 cm^{-1} and a B_g mode located at 190 cm^{-1}.[31] The Raman modes before and after passivation show that capping of the $MoTe_2$ flakes with Al_2O_3 does not degrade their quality as evidenced by the constant line widths of the 2H E_{2g} peak (6.5 cm^{-1}) and the 1T′ A_{1g} peak at 126 cm^{-1} (7.5 cm^{-1}).[24,32] XRD scans on the exfoliated films shown in Fig. 2(b) correspond well to the literature and further validate the monocrystalline nature of the exfoliated films.[13]

Initially, bare 2H and 1T′-$MoTe_2$ films were put in the RTA furnace and subjected to thermal annealing in vacuum. Annealing temperature was varied from 300 °C to 600 °C, with no sign of phase transition. Moreover, at 600 °C, the $MoTe_2$ films degraded. As shown in Fig. 3(a), 2H-$MoTe_2$ flakes show no Raman signal after the 600 °C anneal, which proves that an encapsulation layer is necessary to protect $MoTe_2$ from decomposition during high temperature treatments. This agrees with published reports where 2H-$MoTe_2$ has been passivated with monolayer graphene for high temperature experiments to protect it from thermal decomposition.[33]

Next, Al_2O_3-capped 2H and 1T′-$MoTe_2$ samples were annealed at high temperatures between 500 and 900 °C. No phase change is observed at temperatures below 900 °C. However, after annealing of

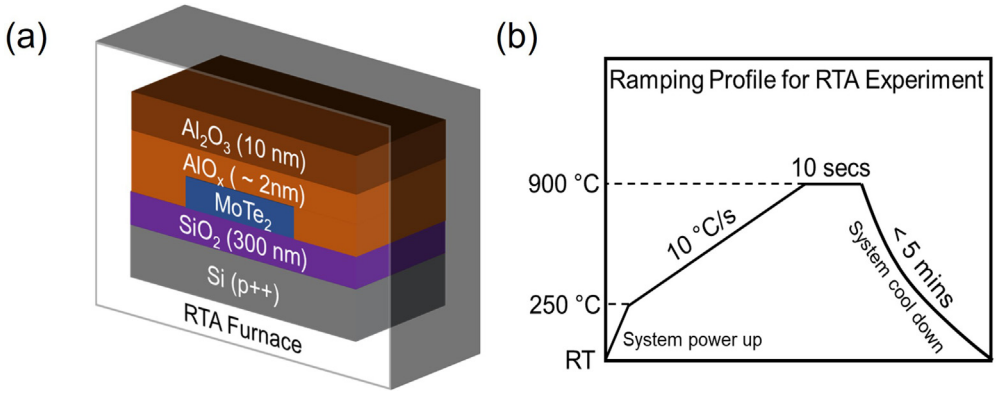

FIG. 1. (a) Cross-sectional schematic of Al_2O_3-encapsulated $MoTe_2$ in the RTA furnace. (b) Temperature profile of the RTA used for phase change experiment.

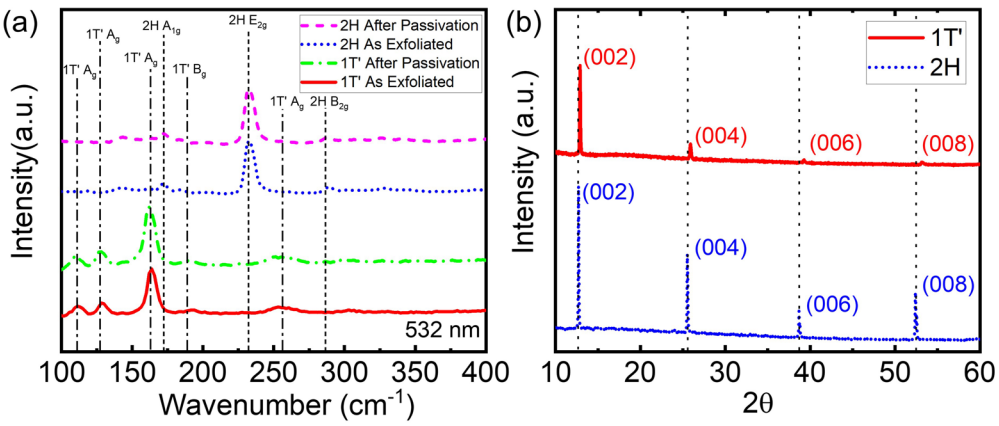

FIG. 2. (a) Raman spectra of pristine 2H and 1T′ $MoTe_2$ before and after Al_2O_3 capping. (b) XRD spectra of pristine 2H and 1T′ flakes.

the capped 2H-$MoTe_2$ films at 900 °C, we observed a structural phase transition from 2H to 1T′. As shown in Fig. 3(b), the 2H E_{2g} and A_{1g} peaks disappear and characteristic 1T′ A_{1g} and B_g peaks appear. The phase transition temperature corresponds well with the phase diagram reported in the literature.[34] The small full width at half maximum (FWHM) of the Raman modes A_g at 126 cm^{-1} (~8.8 cm^{-1}) and B_g at 190 cm^{-1} (~12 cm^{-1}) shows that the resulting 1T′ phase is of high quality.[24] We also performed the annealing experiments both in vacuum at 3×10^{-5} Torr and in N_2 ambient at 10 Torr and achieved the complete phase change in both cases. This shows that ambient pressure does not play a significant role in the phase transition process and that properly passivated $MoTe_2$ phase change devices using inline heaters can be possibly designed for operation at atmospheric conditions. In the literature, claims have been made that laser irradiation[22] and strain engineering[21] can be used to induce phase change between 2H and 1T′. However, measurements by these groups also include Raman peaks at 124 and 138 cm^{-1}, which are similar to the Te metalloid Raman bands arising from sample degradation.[24,35] This raises questions regarding the final product in those samples. In our case, the Raman spectra for fully phase converted 1T′-$MoTe_2$ do not show a signal between 130 and 155 cm^{-1}, which proves that the 1T′ obtained is of high quality and thermal annealing of capped 2H-$MoTe_2$ has not led to sample degradation.

Figure 3(c) shows Raman spectra of Al_2O_3-encapsulated 1T′-$MoTe_2$ annealed at 900 °C for 10 s. According to the $MoTe_2$ phase diagram, the 1T′–2H transition is not expected at this temperature. Instead, we observed peaks at 155 and 242 cm^{-1}, similar to what is reported as the unstable 1T phase by Empante *et al.*[14] and as Mo_6Te_6 by Zhu *et al.*[33] Further investigations are needed to reveal the true nature of the annealed 1T′-$MoTe_2$ films.

To further confirm the absence of sample degradation, we used AFM to monitor the thickness and surface morphology of the $MoTe_2$ thin films throughout the fabrication and annealing processes. Figure 4(a) shows the AFM line scan of a 1.5 nm bilayer 2H-$MoTe_2$[36] film after exfoliation. After capping, the $MoTe_2$ thickness is measured to be (1.5 ± 0.05) nm, which could be due to the roughness in the deposited Al_2O_3. Also, as shown in Fig. 4(b), the $MoTe_2$ flake is conformally covered with Al_2O_3 without formation of islands, as expected when the Al seed layer is used.[29] After annealing at 900 °C, the thickness of the $MoTe_2$ remains the same, which further proves the fact that there is

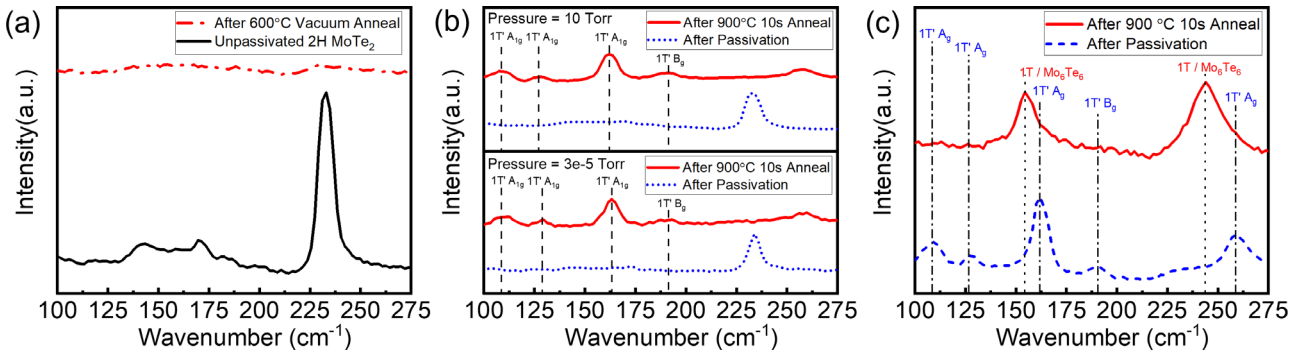

FIG. 3. (a) Raman spectra of bare 2H $MoTe_2$ after 600 °C vacuum anneal. (b) Raman spectra of 2H $MoTe_2$ after 10 s of 900 °C vacuum anneal (3×10^{-5} Torr) and N_2 ambient anneal (10 Torr), showing signs of phase change. (c) Raman spectra of 1T′ $MoTe_2$ after 10 s of 900 °C.

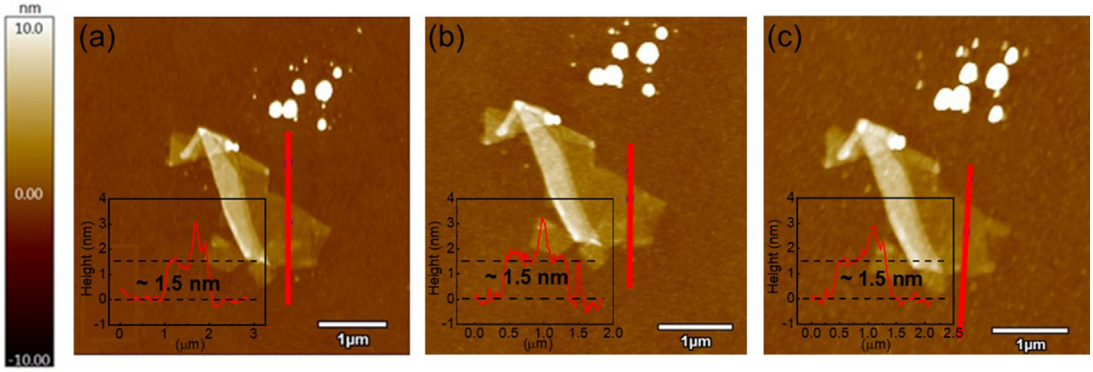

FIG. 4. AFM scan showing height profile of (a) as-exfoliated 2H $MoTe_2$, (b) Al_2O_3 capped 2H $MoTe_2$, and (c) 2H $MoTe_2$ after phase change at 900 °C.

no degradation after the thermal annealing. This is in contrast to the report where a laser was used to attempt phase change from 2H to 1T′,[22,23] which led to sample thinning.[22]

Using AFM, it was also possible to identify exfoliated films of varying thicknesses, namely, ranging from 1.5 to 8 nm. Neither AFM nor Raman indicated a thickness dependence for the temperature required for 2H to 1T′ phase change as shown in Fig. 5. This can be explained by the fact that we are using an RTA furnace for our heating experiments. The RTA heats the entire substrate, which has a larger thermal capacitance compared to the $MoTe_2$ flakes. The use of a dedicated inline heater for the $MoTe_2$ films might introduce thickness dependence on the temperature required for phase transition and may also reduce the time needed for the transition to occur.

In conclusion, we have reported the complete and nondestructive 2H to 1T′ phase change of Al_2O_3-passivated $MoTe_2$ within 10 s using rapid thermal annealing at 900 °C. We have shown that Al_2O_3 passivation plays an important role in the phase change process by preventing flake degradation at high temperatures. No thickness dependence of the transition temperatures was observed for flake thickness ranging from 1.5 to 8 nm. The phase change was also observed both in vacuum and at 10 Torr N_2 ambient pressure, which points to the possibility of operating $MoTe_2$ phase-change devices at atmospheric conditions.

R.S. and S.P. acknowledge funding in part from the National Science Foundation (No. ECCS-1843395). This work was performed, in part, at the North Carolina State University Nanofabrication Facility (NNF) and Analytical Instrumentation Facility (AIF), which are supported by the State of North Carolina and the National Science Foundation (Award No. ECCS-1542015). The NNF and AIF are members of the North Carolina Research Triangle Nanotechnology Network (RTNN), a site in the National Nanotechnology Coordinated Infrastructure (NNCI). S.K. and A.V.D. acknowledge support through the Materials Genome Initiative funding allocated to the National Institute of Standards and Technology.

Certain commercial equipment, instruments, or materials are identified in this paper in order to specify the experimental procedure adequately. Such identification is not intended to imply recommendation or endorsement by the National Institute of Standards and Technology nor is it intended to imply that the materials or equipment identified are necessarily the best available for the purpose.

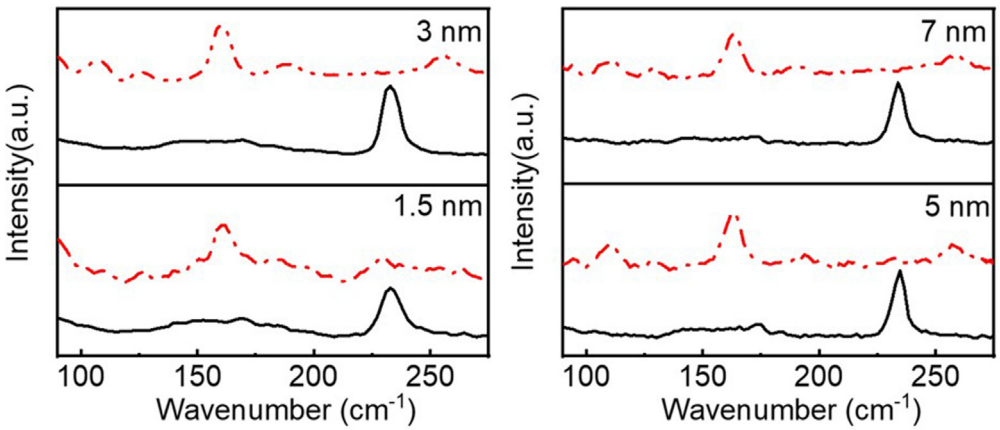

FIG. 5. Raman spectra for 1.5, 3, 5, and 7 nm 2H $MoTe_2$ before heat treatment (solid-black) and after 900 °C heat treatment (dotted-red). The temperature required for phase change is independent of the thickness of the flake.

AUTHOR DECLARATIONS

Conflict of Interest

The authors have no conflicts to disclose.

Author Contributions

Rohan Sengupta: Conceptualization (equal); Data curation (lead); Formal analysis (equal); Methodology (lead); Validation (equal); Writing – original draft (lead); Writing – review and editing (equal). **Saroj Dangi:** Data curation (supporting). **Sergiy Krylyuk:** Formal analysis (equal); Resources (equal); Validation (equal); Writing – review and editing (equal). **Albert V. Davydov:** Formal analysis (equal); Resources (equal); Validation (equal). **Spyridon Pavlidis:** Conceptualization (equal); Formal analysis (equal); Funding acquisition (lead); Project administration (equal); Resources (equal); Supervision (lead); Validation (equal); Writing – original draft (equal); Writing – review and editing (equal).

DATA AVAILABILITY

The data that support the findings of this study are available from the corresponding author upon reasonable request.

REFERENCES

[1] K.-A. N. Duerloo, Y. Li, and E. J. Reed, Nat. Commun. **5**, 4214 (2014).
[2] M. Wuttig and N. Yamada, Nat. Mater. **6**, 824 (2007).
[3] M. Wang, F. Lin, and M. Rais-Zadeh, IEEE Microwave Mag. **17**, 70 (2016).
[4] S. R. Nandakumar, M. Le Gallo, I. Boybat, B. Rajendran, A. Sebastian, and E. Eleftheriou, J. Appl. Phys. **124**, 152135 (2018).
[5] M. Xu, X. Mai, J. Lin, W. Zhang, Y. Li, Y. He, H. Tong, X. Hou, P. Zhou, and X. Miao, Adv. Funct. Mater. **30**, 2003419 (2020).
[6] H. Ryu, Y. Lee, H.-J. Kim, S.-H. Kang, Y. Kang, K. Kim, J. Kim, B. E. Janicek, K. Watanabe, T. Taniguchi, P. Y. Huang, H. Cheong, I.-H. Jung, K. Kim, Y.-W. Son, and G.-H. Lee, Adv. Funct. Mater. **31**, 2107376 (2021).
[7] R. Ma, H. Zhang, Y. Yoo, Z. P. Degregorio, L. Jin, P. Golani, J. Ghasemi Azadani, T. Low, J. E. Johns, L. A. Bendersky, A. V. Davydov, and S. J. Koester, ACS Nano **13**, 8035 (2019).
[8] L. Tao, Y. Zhou, and J.-B. Xu, J. Appl. Phys. **131**, 110902 (2022).
[9] M. Jafari, L. J. Guo, and M. Rais-Zadeh, in *Micro-Nanotechnology Sensors, Systems, and Applications XI* (International Society for Optics and Photonics, 2019), p. 109820W.
[10] Q. Wang, E. T. F. Rogers, B. Gholipour, C.-M. Wang, G. Yuan, J. Teng, and N. I. Zheludev, Nat. Photonics **10**, 60 (2016).
[11] P. Ma, N. Flöry, Y. Salamin, B. Baeuerle, A. Emboras, A. Josten, T. Taniguchi, K. Watanabe, L. Novotny, and J. Leuthold, ACS Photonics **5**, 1846 (2018).
[12] M. B. Vellinga, R. de Jonge, and C. Haas, J. Solid State Chem. **2**, 299 (1970).
[13] D. H. Keum, S. Cho, J. H. Kim, D.-H. Choe, H.-J. Sung, M. Kan, H. Kang, J.-Y. Hwang, S. W. Kim, H. Yang, K. J. Chang, and Y. H. Lee, Nat. Phys. **11**, 482 (2015).
[14] T. A. Empante, Y. Zhou, V. Klee, A. E. Nguyen, I. H. Lu, M. D. Valentin, S. A. Naghibi Alvillar, E. Preciado, A. J. Berges, C. S. Merida, M. Gomez, S. Bobek, M. Isarraraz, E. J. Reed, and L. Bartels, ACS Nano **11**, 900 (2017).
[15] J. C. Park, S. J. Yun, H. Kim, J.-H. Park, S. H. Chae, S.-J. An, J.-G. Kim, S. M. Kim, K. K. Kim, and Y. H. Lee, ACS Nano **9**, 6548 (2015).
[16] P. Tsipas, S. Fragkos, D. Tsoutsou, C. Alvarez, R. Sant, G. Renaud, H. Okuno, and A. Dimoulas, Adv. Funct. Mater. **28**, 1802084 (2018).
[17] Y. Wang, J. Xiao, H. Zhu, Y. Li, Y. Alsaid, K. Y. Fong, Y. Zhou, S. Wang, W. Shi, Y. Wang, A. Zettl, E. J. Reed, and X. Zhang, Nature **550**, 487 (2017).
[18] D. Zakhidov, D. A. Rehn, E. J. Reed, and A. Salleo, ACS Nano **14**, 2894 (2020).
[19] A. Nipane, D. Karmakar, N. Kaushik, S. Karande, and S. Lodha, ACS Nano **10**, 2128 (2016).
[20] C. J. McClellan, E. Yalon, K. K. H. Smithe, S. V. Suryavanshi, and E. Pop, ACS Nano (2021).
[21] S. Song, D. H. Keum, S. Cho, D. Perello, Y. Kim, and Y. H. Lee, Nano Lett. **16**, 188 (2016).
[22] S. Cho, S. Kim, J. H. Kim, J. Zhao, J. Seok, D. H. Keum, J. Baik, D.-H. Choe, K. J. Chang, K. Suenaga, S. W. Kim, Y. H. Lee, and H. Yang, Science **349**, 625 (2015).
[23] Y. Tan, F. Luo, M. Zhu, X. Xu, Y. Ye, B. Li, G. Wang, W. Luo, X. Zheng, N. Wu, Y. Yu, S. Qin, and X.-A. Zhang, Nanoscale **10**, 19964 (2018).
[24] S.-Y. Chen, C. H. Naylor, T. Goldstein, A. T. C. Johnson, and J. Yan, ACS Nano **11**, 814 (2017).
[25] W. Hou, A. Azizimanesh, A. Sewaket, T. Peña, C. Watson, M. Liu, H. Askari, and S. M. Wu, Nat. Nanotechnol. **14**, 668 (2019).
[26] H. Nan, J. Jiang, S. Xiao, Z. Chen, Z. Luo, L. Zhang, X. Zhang, H. Qi, X. Gu, X. Wang, and Z. Ni, Nanotechnology **30**, 034004 (2018).
[27] F. Zhang, H. Zhang, S. Krylyuk, C. A. Milligan, Y. Zhu, D. Y. Zemlyanov, L. A. Bendersky, B. P. Burton, A. V. Davydov, and J. Appenzeller, Nat. Mater. **18**, 55 (2019).
[28] P. Borodulin, N. El-Hinnawy, C. R. Padilla, A. Ezis, M. R. King, D. R. Johnson, D. T. Nichols, and R. M. Young, in *2017 IEEE MTT-International Microwave Symposium* (IEEE, 2017), pp. 285–288.
[29] S. Son, S. Yu, M. Choi, D. Kim, and C. Choi, Appl. Phys. Lett. **106**, 021601 (2015).
[30] C. Ruppert, O. B. Aslan, and T. F. Heinz, Nano Lett. **14**, 6231 (2014).
[31] R. Beams, L. G. Cançado, S. Krylyuk, I. Kalish, B. Kalanyan, A. K. Singh, K. Choudhary, A. Bruma, P. M. Vora, F. Tavazza, A. V. Davydov, and S. J. Stranick, ACS Nano **10**, 9626 (2016).
[32] F. Ye, J. Lee, J. Hu, Z. Mao, J. Wei, and P. X.-L. Feng, Small **12**, 5802 (2016).
[33] H. Zhu, Q. Wang, L. Cheng, R. Addou, J. Kim, M. J. Kim, and R. M. Wallace, ACS Nano **11**, 11005 (2017).
[34] T. B. Massalski, H. Okamoto, P. R. Subramanian, and L. Kacprzak, ASM Int. **1990**, 2104.
[35] L. Yang, H. Wu, W. Zhang, Z. Chen, J. Li, X. Lou, Z. Xie, R. Zhu, and H. Chang, Nanoscale **10**, 19906 (2018).
[36] Q. Wang, J. Chen, Y. Zhang, L. Hu, R. Liu, C. Cong, and Z.-J. Qiu, Nanomaterials **9**, 756 (2019).